Practical Thoughts on Using Repeated Bipolar Gradients for MR-ARFI

J. Chen[1,2], and K. Butts Pauly[2]

[1]Electrical Engineering, Stanford University, Stanford, CA, United States, [2]Radiology, Stanford University, Stanford, CA, United States

Introduction MR acoustic radiation force imaging (MR-ARFI) is a promising monitoring method for some high intensity focused ultrasound (HIFU) treatments. Instead of measuring the temperature increase induced by the sonication, MR-ARFI uses motion sensitizing gradients to detect the displacement introduced by the acoustic radiation force (1). The most attractive feature of MR-ARFI is that it could localize the displacement while sonicating at very low duty cycle, e.g. less than 5%. Therefore, it could potentially be used for safety verification of HIFU thermal ablation, and monitoring HIFU mechanical treatments, including HIFU induced blood-brain-barrier disruption and targeted drug delivery (2). However, for these purpose, the displacement measurement must be accurate and precise. Since the displacement is on the order of 1 μm, the displacement encoding (DE) gradient must be applied at the maximum amplitude to gain enough encoding sensitivity. Conventional MR-ARFI sequence uses a pair of Stejskal Tanner gradients (unipolar, Fig.1 DE(A)) for encoding. Unfortunately, large unipolar gradients may render the image susceptible to eddy currents and signal loss from diffusion. Our previous work has shown that using repeated bipolar gradients (Fig.1 DE(B)) as the DE gradient can significantly improve the accuracy and precision of the displacement map at no cost of scan time or encoding sensitivity. A typical displacement map is displayed in Fig.2, with a displacement of ~0.4 μm at the focal spot. In this work, we continue the initial work and provide some practical thoughts on using the repeated bipolar gradients for MR-ARFI.

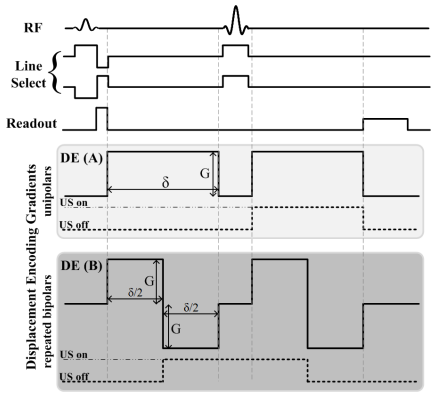

Fig.1 Two motion encoding gradient sets for comparison. The sonication schemes are illustrated by the dotted lines.

Fig.2 An example of the displacement map acquired with the repeated bipolar gradients.

Methods The first consideration is the bulk motion sensitivity of the different encoding gradients. For comparison, imaging was performed with a line scan sequence (3) (TR/TE=500/69 ms, FOV=24×3 cm, matrix size=256×31, slice thickness=5 mm, bandwidth=7.81 kHz, nex=5, encoding amplitude G=4 G/cm, encoding pulse width δ=18 ms) on a 3T GE Signa MR scanner. Two pairs of images were acquired with the unipolar or repeated bipolar gradients, respectively. Each pair was acquired by the opposite polarity of the DE gradients, and then subtracted to see the phase variation caused by the bulk motion. Linear fitting was performed along the readout direction for each line of the phase difference.

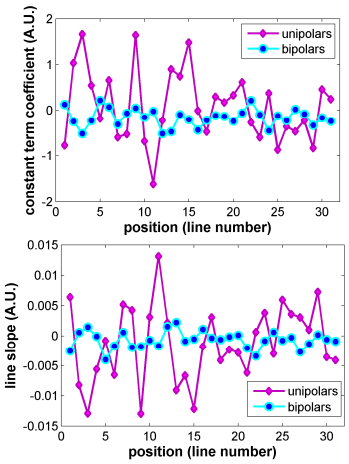

Fig.3 Linear fitting result of each line of the phase difference image, demonstrating the robustness of the bipolar gradients against bulk motion.

The second consideration is the optimized encoding width δ. It has been shown that the signal-to-noise ratio (SNR) of the displacement map is a function of the encoding width δ (4). For the repeated bipolars, it is expressed by

$$SNR_{d,bi}(\delta) = \sqrt{2}\frac{A}{\sigma} d \cdot 4\pi\gamma G\delta \cdot \exp\left(-\frac{1}{6}\gamma^2 G^2 \delta^3 D\right)\exp\left(-\frac{2\delta + const}{T2}\right)$$, where

D is the diffusion coefficient of the object, A/σ is the SNR of the magnitude image without diffusion or T2 weighting, d is the radiation force induced displacement, and *const* is a small time constant based on the sequence design. A simulation based on this equation was performed for 4 tissue types with different T2 and apparent diffusion coefficient (ADC) (5-7) to look for the optimized δ.

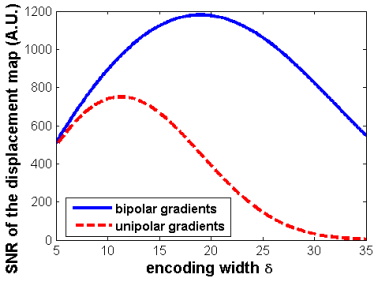

Fig.4 SNR simulation of the white matter. The repeated bipolar improves the SNR compared to the unipolar set with an optimized pulse width of 19 ms.

Results Since the phantom was placed on the scanner table during the image acquisition, the vibration of the scanner introduced constant and linear phase accumulation on the phase difference. As demonstrated in Fig.3, the linear fitting results of the repeated bipolar gradient are an order of magnitude smaller than those of the unipolar gradient. The repeated bipolar gradients are more robust against random bulk motion without any lost of the sensitivity towards radiation force induced motion.

The computer simulation of displacement SNR is shown in Fig.4 using the apparent diffusion coefficient (ADC) and T2 values of white matter (Table 1). Comparing the result of the unipolar gradients, SNR was significant enhanced by the repeated bipolar gradients, with a maximized SNR at the encoding width of 19 ms. This pulse width is the optimized pulse width for displacement SNR consideration. The same method was applied to other tissue types, including kidney, liver, and prostate, with the calculated optimized encoding widths shown in Table 1.

Discussion This study analyzes two aspects in the clinical applications of MR-ARFI. In *in vivo* applications, the total bulk motion will have contributions from many sources besides the scanner vibration, including patient respiration and blood pulsation. Since these can lead to irrecoverable signal loss (8), it is important to minimize the sensitivity to bulk motion, as demonstrated by the repeated bipolar DE gradient set. The second aspect analyzed here is the optimization due to the encoding width δ. Higher sensitivity encoding requires a longer δ, but at the cost of image SNR and higher measurement uncertainty. The optimized δ is a function of tissue type and recommended values for different tissue types are listed in Table 1.

Table 1. Optimized encoding pulse width using the repeated bipolar gradients for

Tissue Type	T2 (ms)	ADC (10^{-3} mm^2/s)	Optimized δ (ms)
White matter	92	1.5 (parallel dir)	**19**
Kidney	58	1.63	**16.6**
Liver	43	0.69	**17.2**
Prostate	74	1.64	**17.8**

Acknowledgements This work was supported by NIH RO1 CA111981, RO1 CA121163 and P41 RR009784.

Reference 1) McDannold et al, Med Phys 2008;35:3748-3758
2) Treat et al, Int J Cancer 2007;121:901-90
3) Gudbjartsson et al, MRM 1996;36:509-519
4) Chen et al, 7th IMRI symposium 2008
5) Nishimura, EE369B course reader
6) Tien et al, AJR 1994;162:671-677
7) Namimoto et al, Radiology 1997;204:739-744
8) Wedeen et al, MRM 1994;32(1):116-20.